Nonlinearity in bacterial population dynamics: Proposal for experiments for the observation of abrupt transitions in patches

V. M. Kenkre[1] and Niraj Kumar

Consortium of the Americas for Interdisciplinary Science and Department of Physics and Astronomy, University of New Mexico, Albuquerque, NM 87131

Edited by Harry L. Swinney, University of Texas, Austin, TX, and approved October 8, 2008 (received for review May 28, 2008)

An explicit proposal for experiments leading to abrupt transitions in spatially extended bacterial populations in a Petri dish is presented on the basis of an exact formula obtained through an analytic theory. The theory provides accurately the transition expressions despite the fact that the actual solutions, which involve strong nonlinearity, are inaccessible to it. The analytic expressions are verified through numerical solutions of the relevant nonlinear equation. The experimental setup suggested uses opaque masks in a Petri dish bathed in ultraviolet radiation [Lin A-L, *et al*. (2004) *Biophys J* 87:75–80 and Perry N (2005) *J R Soc Interface* 2:379–387], but is based on the interplay of two distances the bacteria must traverse, one of them favorable and the other adverse. As a result of this interplay feature, the experiments proposed introduce highly enhanced reliability in interpretation of observations and in the potential for extraction of system parameters.

bacteria in Petri dish | Fisher equation

Phenomena displaying abrupt transitions are of special interest to a variety of sciences, including physics and biology. In some physical cases they arise from cooperative interactions among a large number of constituents (e.g., molecules or spins), and in others from nonlinearities in interaction inherent in the system (e.g., in some mechanical systems with only a few degrees of freedom). In the first form they are known as phase transitions (1), in the second, as bifurcations (2). Abrupt phenomena also command attention in the context of extinction of populations, a subject of obvious interest to biology (3). Transitions in populations, therefore, constitute an exciting topic of interdisciplinary science combining physics and biology, and this article reports a theory and proposes an experiment in this topic. The special feature of the proposed experiment is that it may be performed with relatively simple equipment and measurement techniques.

The system to be considered consists of bacteria in a Petri dish, allowed to grow and move, spatial selection being imposed via lethal ultraviolet radiation that is incident on the dish, but punctuated by opaque masks that protect the bacteria in chosen regions. Experiments under such a setup were initiated several years ago by Lin *et al*. (4, 5) who used moving masks in response to a theoretical analysis (6, 7) that focused on spatial disorder. A quite different experiment using stationary masks of varying sizes, and employing bacterial extinction as the key phenomenon, was then proposed (8). That proposal was carried out experimentally (9) and the predictions of ref. 8 were verified. Related investigations on this topic may be found in refs. 10–12, the general problem of bacterial dynamics in Petri dishes has been addressed in various articles and contexts (13, 14).

The underlying assumption behind most of these studies is that the bacteria obey a simple Fisher equation (15) for the time evolution of their dynamics, their population density $u(x,t)$, where x is the position in a 1-dimensional space (the linear dimension of the Petri dish), and t is the time, being governed by

$$\frac{\partial u(x)}{\partial t} = D\frac{\partial^2 u(x)}{\partial x^2} + au(x) - bu^2(x). \qquad [1]$$

Here, a and b are, respectively, the growth rate and a competition parameter arising from the resources being limited, and D is the bacterial diffusion constant.

Eq. **1** generally does not permit analytic solutions for arbitrary times but can be solved in the steady state explicitly in terms of Jacobian elliptic functions, if the bacterial population is assumed to vanish at the edges of a finite region. Physically, this could correspond to an idealization in which, although the mask protects the bacteria from the lethal effects of the ultraviolet radiation, the latter is so potent that the bacterial population must vanish everywhere outside the mask where the radiation impinges on the bacteria. Mathematically, these are Dirichlet boundary conditions. The elliptic function solution, given independently in a recent analysis (8), but known decades earlier through the work of Skellam (16), and elucidated in textbooks (18), leads to the well-known KISS transition (17): the steady-state bacterial population vanishes for any width of the mask lower than a critical value that, interestingly, depends on the diffusion constant D and the growth rate a, but not on the nonlinearity parameter b. The specific expression for the critical mask width is $\pi\sqrt{D/a}$. Combining this expression with information about bacterial diffusion constants and growth rates discussed by Mann (11), Kenkre and Kuperman calculated the critical mask width to be ≈ 0.5 cm, and suggested that an experiment be carried out to observe the transition. Perry (9) followed the suggestion, and reported observing a transition width of 0.8 cm in his experiments on a nonchemotactic strain RP9535 of *Escherichia coli* bacteria. Because the Dirichlet boundary condition is only an extreme idealization, Perry argued, appropriately, that it is preferable to invoke the analysis of Ludwig *et al*. (19) for quantitative verification. That analysis assumes that the growth rate a is negative in the region outside the mask (and of magnitude a_1), rather than infinite as would correspond to Dirichlet boundary conditions, and arrives at the critical mask width as being $L = 2\sqrt{D/a}\arctan\sqrt{a_1/a}$. The Dirichlet expression is recovered from this Ludwig formula if the effect of the ultraviolet radiation outside the mask is "infinitely" lethal.

Proposal for Experiment

Need for the experimental proposal that we present here arises because the stationary single-mask experiment (8, 9) uses for its interpretation a number of inputs that suffer from a certain degree of uncertainty. Some of these uncertainties are about the values of D and a (11), and others are about the extent to which other phenomena, such as signaling (9), that occur in bacterial movement might affect the outcome of the experiment. Because

Author contributions: V.M.K. designed research; V.M.K. and N.K. performed research; V.M.K. and N.K. contributed new reagents/analytic tools; and V.M.K. wrote the paper.

The authors declare no conflict of interest.

This article is a PNAS Direct Submission.

[1]To whom correspondence should be addressed. E-mail: kenkre@unm.edu.

This article contains supporting information online at www.pnas.org/cgi/content/full/0805215105/DCSupplemental.

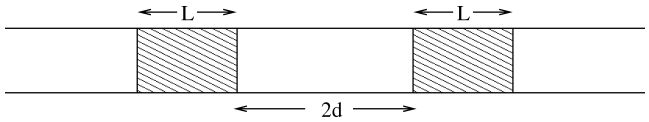

Fig. 1. Our proposed experimental setup showing two favorable regions each of length L separated by a hostile region of length $2d$. The focus of observation is the interdependence of the critical values of L and d at which extinction occurs.

absolute values of critical lengths may be difficult to obtain with an acceptable degree of accuracy, we propose here stationary mask observations that focus, instead, on the *interdependence of two critical lengths*. The essential feature of this present proposal is to have more than one mask in the Petri dish, so that there are two controllable lengths, a favorable length associated with a livable region for the bacteria, and a hostile length associated with an unlivable region. The double control possible in the proposed experiment opens the prediction space from a single value to an infinity of values. The variation of the critical value of one of the lengths when the other is changed presents an entire *relationship* that is directly observable, rather than a single value, and therefore could lead to a much cleaner and more trustworthy interpretation of the observations.

The simplest system to study consists of two masks, each of length L, separated by a distance of length $2d$ as shown in Fig. 1. The previously investigated case with a single mask (8, 9) corresponds, obviously, to infinite d. To test the idea behind the new proposal, we carried out numerical studies of the full nonlinear Fisher Eq. **1** with given values of D, a, a_1, and b (10, 0.1, −0.9 and 1 in appropriate units). All lengths were expressed as ratios to the diffusion length $\sqrt{D/a}$. The numerical studies used an explicit finite differences scheme, x being discretized in intervals of 0.1. The convergence to a steady state was analyzed by measuring the distance between successive solutions.

The result we found (see Fig. 2) is that the critical value of the mask width L, that is, the smallest value that can support a nonzero bacterial population in the steady state, is lowered for a finite intermask distance d. We considered 10 different values of the hostile length (the intermask distance d) and varied the favorable length (the mask width L.) For each L–d pair, we started with arbitrary initial conditions and let the program run until no time dependence was discernible. We repeated the procedure for each of several sufficiently low values of L and increased L until the extinction disappeared. We also reversed the procedure starting with high values of L and decreased them systematically until extinction appeared. Numerous runs allowed us to obtain corresponding pairs of L and d that mark the transition region. The results are denoted by filled circles in Fig. 2. The shaded area represents the extinction region and the unshaded area the parameter region in which bacterial population densities are nonzero in the steady state. The curve passing through the numerically found transition points may be considered, at this stage of our discussion, to be simply a smooth joining trace. We will see below that its exact shape can be accessed through our analytic theory.

It is easy to understand, on the basis of a qualitative argument, the shape and tendency of the results of the numerical solutions of the nonlinear equation. Bacteria diffuse from within the mask to the harsh region and die if they reach that region. Small values of the mask width or large values of the intermask distance result in extinction. The extinction effect is worsened by an increase in the intermask distance for small values of that distance, but the effect saturates for larger values. Hence, the saturation in the curve.

All of these features can be tested experimentally in our proposed setup. Quantitative comparison with the predictions of the Fisher equation are possible because we have developed an exact analytic theory of the interplay of the favorable and hostile distances as reflected in the transition. What makes the proposed comparison with experiment significant is that, although the Fisher equation, whose *numerical* solution has led us to set out the separation curve between the extinction region and the rest in Fig. 2, cannot be solved exactly by analytic means, the separation curve itself can be obtained analytically. Indeed, we show below that the curve is given precisely by

$$L = \sqrt{\frac{D}{a}}\left[\arctan\sqrt{\frac{a_1}{a}} + \arctan\left[\sqrt{\frac{a_1}{a}}\tanh\left(d\sqrt{\frac{a_1}{D}}\right)\right]\right]. \quad [2]$$

This prediction, which is one of the central analytic results of this article, coincides with the solid curve in Fig. 2.

Analytic Theory for the Twin Mask Setup

Following the ideas of Ludwig *et al*. (19), but applying them to the many-mask system, we consider the steady state of the Fisher Eq. **1** and argue that, if there is a transition, the quadratic term in the steady state $u(x)$ can be neglected at the extinction point in favor of the linear terms because $u(x)$ itself vanishes at the transition. We are thus led to seek the solutions of

$$\frac{d^2u(x)}{dx^2} + \alpha^2 u(x) = 0 \quad [3]$$

under the two masks, and of

$$\frac{d^2u(x)}{dx^2} - \alpha_1^2 u(x) = 0 \quad [4]$$

outside the masks, with $\alpha^2 = a/D$ and $\alpha_1^2 = a_1/D$. We take the masks to lie from $x = \pm d$ to $x = \pm(d + L)$. By using I and O as constants, the most general functions for $u(x)$ inside and outside the mask, respectively, are, as a result of the symmetry (we consider only the right side of the origin, because all considerations repeat unchanged on the left side by symmetry)

$$u(x) = I\cos(\alpha|x| - \phi) \quad [5]$$

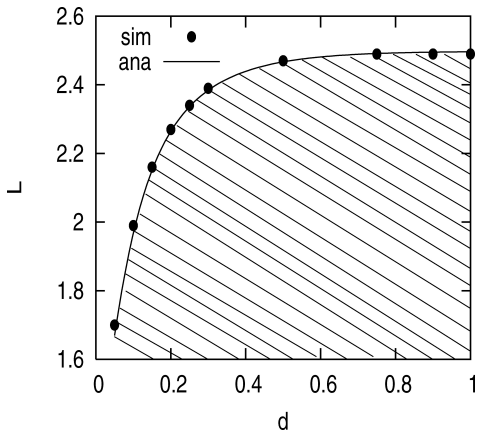

Fig. 2. Basis of the experimental proposal. Shown is the interdependence of the critical values of the favorable and hostile lengths L and d, respectively. The former is the width of the mask and the $2d$ is the distance between the two masks (see Fig. 1), both lengths being expressed in this plot in units of the diffusion length $\sqrt{D/a}$, where a is the growth rate under the masks. Outside the masks a is replaced by $-a_1$ to represent the harsh effect of the ultraviolet light, the magnitude of a_1 being taken, for the purposes of this plot, to be 9 times that of a. We solved Eq. **1** numerically for various different values of the nonlinear parameter b and found that the results did not depend on those values provided b was nonzero and positive. The shaded region represents pairs of L and d values that lead to bacterial extinction in the steady state. Filled circles mark the onset of extinction and are obtained from the numerical solution. The solid line, constructed simply to smoothly join the circles, is found to coincide precisely with the prediction of our analytic theory.

BIOPHYSICS

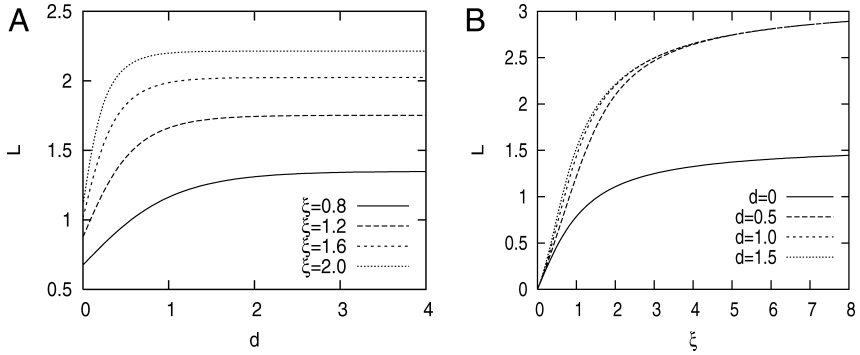

Fig. 3. Our analytic predictions for the dependence of critical values of the favorable length L and the hostile length d, respectively, from Eq. **2**. The lengths are expressed as dimensionless ratios to the diffusion length $\sqrt{D/a}$. (*A*) Different curves correspond, as shown in the legend, to different values of ξ, i.e., to different intensities of the ultraviolet radiation. Note the doubling of L as d passes from 0 to ∞ in all curves. (*B*) The dependence of L on the ultraviolet radiation intensity is shown for various values of d. All d values produce the same saturation values of L for infinitely harsh ultraviolet intensity except for $d = 0$ for which the saturation value is one half that of the others. See text for explanation.

inside the mask, $d < x < d + L$,

$$u(x) = O \exp(-\alpha_1 |x|) \quad \textbf{[6]}$$

in the extreme outside, in the harsh region, $x > d + L$, and

$$u(x) = C \cosh(\alpha_1 |x|) \quad \textbf{[7]}$$

in the central region between the two masks, $-d < x < d$. Matching the logarithmic derivative of the solution at the outer and the inner boundaries leads to

$$\tan[\alpha(d + L) - \phi] = \alpha_1/\alpha$$
$$\tan(\alpha d - \phi) = -(\alpha_1/\alpha) \tanh \alpha_1 d,$$

and elimination of ϕ from these two equations leads to Eq. **2** quoted above. Notice how, in light of the behavior of the hyperbolic tangent, Eq. **2**, one of our central results, reduces to Ludwig *et al*.'s (19) single-mask value of L, when d attains infinite values, and half that value when d vanishes. Both are fully expected and natural results. It is also instructive to rewrite the transition relation as

$$\mathcal{L} = \arctan \xi + \arctan(\xi \tanh \delta\xi) \quad \textbf{[8]}$$

where we express the favorable distance L and hostile distance d normalized to the growth diffusion length $g = \sqrt{D/a}$ as $\mathcal{L} = L/g$ and $\delta = d/g$, respectively, and the depletion parameter ξ is the square root of the ratio of the destruction rate a_1 and the growth rate a.

We display in Fig. 3*A* our analytic result, Eq. **2**, equivalently Eq. **8**. As in other plots the lengths are expressed as dimensionless ratios to the diffusion length $\sqrt{D/a}$. Different curves correspond, as shown in the legend, to different values of ξ, i.e., to different intensities of the ultraviolet radiation. The curve for $\xi = 3$ from our theory is shown as the solid line in Fig. 2 and displays exact coincidence with the numerical findings. Note that the numerical solutions are of the full nonlinear equation and have been found for a specific b, whereas the analytic theory is linear and does not require the use of a value of b, requiring for its application only the condition $b > 0$.

It is clear from our Eq. **2** that the variation of the destructive rate a_1 may also be employed for useful experimental exploration, at least in principle. Although this could have also been done in the one-mask scenario of ref. 9, we explain the idea here in the two-mask case. Additional confirmation of the theoretical picture of the dynamics of the bacteria might be provided by observing how the critical L–d values change with the *intensity* of the ultraviolet light. Even if we do not know the precise dependence of a_1 on the intensity, we can be fairly certain that it increases with the latter, and undergoes a saturation at high values of the intensity. A variation of the critical value of L with the intensity would therefore show qualitative behavior similar to the variation with a_1, equivalently with the ratio $\xi = \sqrt{a_1/a}$. The latter variation is displayed in Fig. 3*B*. With one exception, all d values produce the same saturation value of L for large ξ. The exception is $d = 0$: its saturation value is one half that of the others. Mathematically, this corresponds to the hyperbolic tangent becoming 1 for all nonzero values of d for large enough ξ, but vanishing if d vanishes. Physically, this means that, if there is an adverse region between the masks, bacteria will be killed on arriving there, in light of the infinitely harsh radiation, reducing the problem to a single-mask scenario with the given L as the mask width. However, if the intermediate harsh region does not exist at all (because $d = 0$), one is reduced to considering a *single* mask with width twice that of the given mask.

Our suggestion, thus, is to use both the relative variation of the favorable and hostile lengths, L and d, and of the intensity of ultraviolet light in the manner discussed, to check our simple quantitative predictions.

Multiple Mask Setup and Circular Petri Dish

It is possible and useful to construct setups with *multiple* masks for further experimental verification. The theory for this situation along the arguments of Ludwig *et al*. (19) that we have developed here is slightly more tedious to write down. For ease in notation, let us adopt as we did in Eq. **8**, the symbols $\mathcal{L}$ and δ to express the favorable and hostile lengths in units of $\sqrt{D/a}$. Then, the linear Petri dish formula for an even number of masks is obtained by executing the following pseudocode.

Let H be an operator defined by the successive operations of (*i*) taking the hyperbolic tangent of what it acts on, (*ii*) multiplying the result by ξ, (*iii*) taking the arctangent of the result, and (*iv*) subtracting the result from $\mathcal{L}$. Define the operator T similarly through the successive operations of (*i*) taking the trigonometric tangent of what it acts on, (*ii*) dividing the result by ξ, (*iii*) taking the hyperbolic arctangent of the result, and (*iv*) subtracting the result from $2\xi\delta$.To obtain the required formula for an even number of masks, start with the product $\xi\delta$. Apply H and then T alternately and successively so that there are as many Hs in the operation as the number of mask pairs in the system, but one more H than T. (Thus, do H for a pair of masks, HTH for 4 masks, $HTHTH$ for 6 masks, and so on.) Finally, equate the result to the arctangent of ξ to get an implicit formula showing the $\mathcal{L}$–δ relation. The pseudocode can be expressed succinctly in terms of operators T and H by stating that the general expression for $2n$ masks can be formally written as $[H \prod_{i=1}^{n-1} (TH)_i](\xi\delta) = \arctan \xi$. As can be

verified, this reproduces the 2-mask formula, Eq. **2**. The 4-mask formula is

$$\mathcal{L} = \arctan\xi + \arctan(\xi\tanh(2\xi\delta - \operatorname{arctanh}((1/\xi)\tan(\mathcal{L} - \arctan(\xi\tanh\xi\delta))))). \quad [9]$$

Our suggested setup and calculations have taken the Petri dish to have infinite extension away from the two masks, an assumption that should be reasonable in light of the destructive effects of the radiation. We have also analyzed another practical extension of the theory. Consider the 2-mask situation in a *circular* Petri dish, i.e., one in which the boundary conditions are periodic, the hostile distance between the edges of the masks being $2d$ on one side as in the earlier analysis, but now also $2R$ on the other side. Let the width of the dish be small enough so that bacterial diffusion can be considered to still be 1-dimensional but over a total distance of extent $2(L+d+R)$. We are not interested, here, in 2-dimensional considerations appropriate to wide dishes, an example of which may be found in ref. 20 for experiments with *moving* masks or rotating dishes.

It is now possible to arrive at

$$L = \sqrt{\frac{D}{a}}\left(\arctan\left(\sqrt{\frac{a_1}{a}}\tanh\left(R\sqrt{\frac{a_1}{D}}\right)\right) + \arctan\left(\sqrt{\frac{a_1}{a}}\tanh\left(d\sqrt{\frac{a_1}{D}}\right)\right)\right) \quad [10]$$

for the 2-mask case, at

$$L = 2\sqrt{\frac{D}{a}}\arctan\left(\sqrt{\frac{a_1}{a}}\tanh(\alpha_1 R)\right) \quad [11]$$

for the single-mask case as a generalization of the Ludwig formula for the circular dish, and, with $\mathcal{R} = R\sqrt{a/D}$, at

$$\mathcal{L} = \arctan(\xi\tanh\xi\mathcal{R}) + \arctan(\xi\tanh(2\xi\delta - \operatorname{arctanh}((1/\xi)\tan(\mathcal{L} - \arctan(\xi\tanh\xi\delta))))) \quad [12]$$

for the combination of the multiple-mask setup (here, a 4-mask example) in a circular Petri dish. Further details, including the manner of derivation and a pictorial representation, may be found in supporting information (SI) *Appendix*.

Chemotaxis Effects

In his verification of the theoretical predictions (8) of bacterial extinction, Perry (9) has stated that he performed his experiments by using the strain RP9535 of *E. coli* bacteria because, in contrast to the strain RW120 used by Lin *et al*. (4, 5), RP9535 does not exhibit chemotaxis effects. The analysis we have presented above applies, in the form given, to the RP9535 strain and all other strains in which chemotaxis is absent or negligible. It is interesting to ask what modifications would be required if chemotaxis is at work. We address this question very briefly here.

Chemotaxis involves repulsion or attraction of the bacteria relative to another entity such as nutrients or waste. A typical theoretical construct (21–24) for its description involves the coupled equations

$$\frac{\partial u}{\partial t} = D\frac{\partial^2 u}{\partial x^2} + A\frac{\partial}{\partial x}\left(u\frac{\partial c}{\partial x}\right) + au - bu^2,$$
$$\frac{\partial c}{\partial t} = D_c\frac{\partial^2 c}{\partial x^2} + hu - kc, \quad [13]$$

that govern $c(x,t)$, the density of wastes or nutrients, in addition to the bacterial density $u(x,t)$. In keeping with the experimental setup that we have proposed, we consider here waste produced by the bacteria as the additional entity in the chemotactic interaction. The bacteria will be now assumed to perform a random walk (move diffusively) but in a manner biased away from the waste

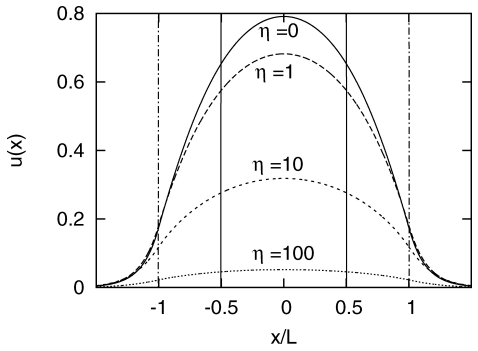

Fig. 4. Chemotaxis effects on the steady-state density profile showing enhanced depletion within the mask. Plotted is the bacterial density $u(x)$ at steady state, in units of a/b, as a function of the distance x expressed in units of the critical length L. Solid vertical lines mark that L; dash-dotted lines mark the (larger than critical) width of the mask for which the plots are constructed. Several values of the chemotactic interaction parameter $\eta = \alpha a/Db$ are considered. The larger the η, the greater the depletion.

that they produce at their own location at rate h. The waste itself might diffuse with diffusion constant D_c, and be removed out of the region at rate k. It is easy to show (23) that, if waste diffusion is important to consider and the decay rate k is negligible, one obtains a Burger's equation (augmented by the reaction diffusion terms in the u equation above). The situation in the experiments (4, 5, 9) considered here appears to be the opposite. The waste is known (11) to drop down from the surface where the bacterial diffusion occurs and then disappear from the region under description. Thus, it seems appropriate to consider $D_c = 0$. If the removal of the waste matter happens faster than the dynamics of the bacteria, we may use a timescale disparity argument to derive a single closed equation for the bacterial density,

$$\frac{\partial u}{\partial t} = \frac{\partial}{\partial x}\left[(D + \alpha u)\frac{\partial u}{\partial x}\right] + au - bu^2. \quad [14]$$

Chemotaxis, whose strength is controlled by $\alpha = Ah/k$, simply modifies the Fisher equation by making the diffusion coefficient dependent on the bacterial density u. Eq. **14** clearly shows that its effects will depend on the size of $\alpha u/D$.

We have carried out a number of numerical investigations based on Eq. **14** and on Eq. **13**, as well, and briefly report our findings. First, as shown in Fig. 4, chemotaxis results in a higher effective diffusion constant and, consequently, enhanced depletion of the bacteria within the mask as they move faster into the lethal region. And second, the chemotactic effect completely *disappears* in the context of the *critical* length: the type of chemoaxis we have considered here has no consequence on the analysis of the main body of the article. This is displayed in Fig. 5, specifically in *B*.

It is easy to understand both results from an inspection of Eq. **14**. The consequence of chemotaxis is only to augment the diffusion coefficient of the bacteria by the factor $(1 + \alpha u/D)$, because they are repelled from where they have been. The bacteria under the mask are depleted faster as one increases α, equivalently the dimensionless chemotaxis parameter $\eta = \alpha a/bD$. This can be seen in Fig. 4. It can also be noted in the decrease in the steady-state value observed for supercritical masks in Fig. 5. This explains the first effect. Near the critical region, i.e., near extinction, u is negligible and therefore the chemotactic addition to the diffusion constant has no effect. If the mask width is larger than the critical value L, the extent of the chemotaxis effect can be seen in the value to which the maximum density in the mask settles at long times—the larger the η, the bigger the decrease. But even making the mask width slightly smaller than the value that is critical in the absence of chemotaxis, we ascertain from the plots (Fig. 5*B*) that

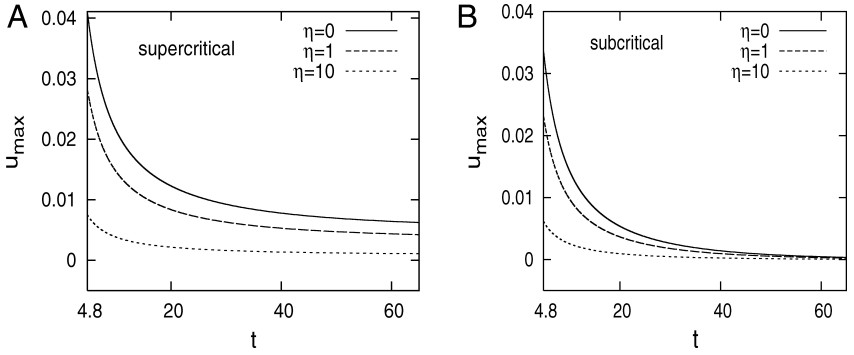

Fig. 5. Absence of chemotaxis effect on the critical length. Plotted is the maximum value u_{max} of the bacterial density within the mask, expressed in units of a/b, as a function of time in units of L^2/D for three values of $\eta = \alpha a/Db = 0, 1, 10$ as shown. For each of the 6 curves shown, u_{max} starts out with the value a/b. That initial portion of the evolution, for $tD/L^2 < 4.8$, is not shown. (*A*) For the supercritical case (mask length slightly larger than the critical length *L*), the density tends to a nonzero value, which is larger, the smaller the chemotactic parameter. (*B*) For the subcritical case (mask length slightly smaller than the critical length *L*), all curves show total depletion. No change thus occurs in the critical length *L* as a consequence of chemotaxis.

chemotaxis has no effect whatsoever on the critical value. This explains the second effect.

We followed the full simulation procedure used to produce Fig. 2 from Eq. **1**, but now from Eq. **14** in the presence of chemotaxis. We employed a semi-implicit scheme, where necessary, to avoid instabilities. Within numerical uncertainties, we found precisely the same curve as in Fig. 2. We also carried out our numerical investigations of extinction with the coupled Eq. **13** to check whether the timescale argument is critical and find that it is not so. These studies confirm our results that chemotaxis affects diffusion but not the critical mask width. Effects of chemotaxis of other kinds on bacterial evolution is a vast subject to which we cannot do justice in this brief analysis. The absence of a chemotaxis effect on the determination of the critical value L that we have shown should be of interest to investigate.

Concluding Remarks

The proposal for experimental observations of abrupt population transitions in patches that we have presented should be of interest for multiple reasons. Patches or spatial inhomogeneities were studied and emphasized early on in ecology by many authors such as Murray (22), Levin (25), and Shigesada and colleagues (26–28) in varied contexts, including traveling waves, and there have been recent contributions as well on the Dirichlet conditions problem for general nonlinearity incorporating Allee effects (29).

Our analysis here provides a clean proposal for experiments that derives its potential for clear interpretation from the use of 2 (or more) controllable distances of travel, one favorable and the other unfavorable. One should be able to use it for extraction of parameter combinations in the Fisher equation, which has been ubiquitous in mathematical ecology. The idea behind the present proposal should therefore find use in systems other than bacterial aggregates. Indeed, we have found similar abrupt transitions in *infected* rodent populations in our study of the Hantavirus epidemic. The theory for that system is, however, more complex, and cannot be developed without approximation. By contrast, the theory we have presented here is, perhaps surprisingly, exact, that is, analytical. This is so despite the fact that analytic solutions of the Fisher equation for these situations do not seem to be possible except as elliptic quadratures. The reason for this happy state of affairs can be understood from the original arguments of Ludwig *et al*. (19), given in their article on spatial patterning of the budworm, or from the lucid explanations given, e.g., in a recent text on mathematical ecology (18). At the transition, the densities vanish and, therefore, terms of order higher than the first may be safely neglected. Our theoretical contribution is only in generalizing that analysis to multiple masks and nonlinear geometries as shown. The observable, controllable features our proposal emphasizes, and directly utilizes, are (*i*) the interplay of the favorable and adverse lengths for bacterial traversal; (*ii*) the variation of the intensity of ultraviolet radiation that changes the interrelationship of the critical values; (*iii*) the multiple-mask setup that reintroduces bacteria into favorable regions after they have passed into arid areas; and (*iv*) the optional use of circular geometry for the Petri dish, which provides one more controllable length.

We have also seen that our results are robust in that they remain unmodified in the presence of at least one type of chemotaxis we have analyzed—involving repulsive interactions of waste material. Our analysis may be extended to other forms of chemotaxis effects, in investigating fluctuation effects (30) that appear from detailed Monte Carlo considerations and become manifest for small population densities, in constructing the theory for transitions in partially infected populations of rodents in open terrains, in analyzing the effects of static disorder in the placement and size of the masks, and in studying the effects of dynamic (time) variation of mask size and placement as in ref. 12. The bacterial experiments proposed above are, however, ready to go and we hope that observations will be made soon along the lines we have discussed.

ACKNOWLEDGMENTS. V.M.K. thanks Gandhi M. Viswanathan for an insightful remark that helped the completion of this work and Marcelo Kuperman for discussions regarding chemotaxis. This work was supported in part by National Science Foundation Grant INT-0336343 and by National Science Foundation/National Institutes of Health Ecology of Infectious Diseases Grant EF-0326757.

1. Stanley HE (1971) *Introduction to Phase Transitions and Critical Phenomena* (Oxford Univ Press, Cambridge, UK).
2. Strogatz SH (1994) *Nonlinear Dynamics and Chaos: With Applications to Physics, Biology, Chemistry and Engineering* (Westview Press, Boulder, CO).
3. Renshaw E (1991) *Modelling Biological Populations in Space and Time* (Cambridge Univ Press, Cambridge, UK).
4. Lin AL, *et al.* (2004) Localization and extinction of bacterial populations under inhomogeneous growth conditions. *Biophys J* 87:75–80.
5. Lin AL (2003) Modern challenges in statistical mechanics: patterns, growth, and the interplay of nonlinearity and complexity. *AIP Conference Proceedings*, eds Kenkre VM, Lindenberg K (American Institute of Physics, Melville, NY), Vol 658.
6. Nelson DR, Shnerb NM (1998) Non-Hermitian localization and population biology. *Phys Rev E* 58:1383–1403.
7. Dahmen KA, Nelson DR, Shnerb NM (2000) Life and death near a windy oasis. *J Math Biol* 41:1–23.
8. Kenkre VM, Kuperman MN (2003) Applicability of the Fisher equation to bacterial population dynamics. *Phys Rev E* 67:051921.
9. Perry N (2005) Experimental validation of a critical domain size in reaction-diffusion systems with *Escherichia coli* populations. *J R Soc Interface* 2:379–387.
10. Wakita J, Komatsu K, Nakahara A, Matsuyama T, Matsushita M (1994) Experimental investigation on the validity of population dynamics approach to bacterial colony formation. *J Phys Soc Jpn* 63:1205–1211.

11. Mann B (2001) Spatial phase-transitions in bacterial growth. PhD thesis (Univ of Texas, Austin, TX).
12. Ballard M, Kenkre VM, Kuperman MN (2004) Periodically varying externally imposed environmental effect on population dynamics. *Phys Rev E* 70:031912.
13. Berg HC (2000) Motile behavior of bacteria. *Phys Today* 53:24–29.
14. Ben-Jacob E, Cohen I, Levine H (2000) Cooperative self-organization of microorganisms. *Adv Phys* 49:395–554.
15. Fisher RA (1937) The wave of advance of advantageous genes. *Ann Eugen London* 7:355–369.
16. Skellam JG (1951) Random dispersal in theoretical populations. *Biometrika* 38:196–218.
17. Kierstead H, Slobodkin LB (1953) The size of water masses containing plankton blooms. *J Mar Res* 12:141–147.
18. Kot M (2003) *Elements of Mathematical Ecology* (Cambridge Univ Press, Cambridge, UK).
19. Ludwig D, Aronson DG, Weinberger HF (1979) Spatial patterning of the spruce budworm. *J Math Biol* 8:217–258.
20. Shnerb NM (2000) Extinction of a bacterial colony under forced convection in pie geometry. *Phys Rev E* 63:011906.
21. Keller EF, Segel LA (1971) Travelling bands of chemotactic bacteria: A theoretical analysis. *J Theor Biol* 30:235–248.
22. Murray JD (1993) *Mathematical Biology* (Springer, Berlin).
23. Brenner MP, Levitov LS, Budrene EO (1998) Physical mechanisms for chemotactic pattern formation by bacteria. *Biophys J* 74:1677–1693.
24. Park S, *et al.* (2003) Influence of topology on bacterial social interaction. *Proc Natl Acad Sci USA* 100:13910–13915.
25. Levin SA (1976) Population dynamic models in heterogeneous environments. *Ann Rev Ecol Syst* 7:287–310.
26. Kinezaki N, Kawasaki K, Takasu F, Shigesada N (2003) Modeling biological invasions into periodically fragmented environments. *Theor Popul Biol* 64:291–302.
27. Shigesada N, Kawasaki K, Teramoto E (1986) Traveling periodic waves in heterogeneous environments. *Theor Popul Biol* 30:143–160.
28. Shigesada N, Kawasaki K (1997) *Biological Invasions: Theory and Practice* (Oxford Univ Press, Oxford, UK).
29. Mendez V, Campos D (2008) Population extinction and survival in a hostile environment. *Phys Rev E* 77:022901.
30. Escudero C, Buceta J, de la Rubia FJ, Lindenberg K (2004) Extinction in population dynamics. *Phys Rev E* 69:021908.

Supporting Information

Nonlinearity in Bacterial Population Dynamics: Proposal for Experiments for the Observation of Abrupt Transitions in Patches

V. M. Kenkre and Niraj Kumar
Consortium of the Americas for Interdisciplinary Science and Department of Physics and Astronomy, University of New Mexico, Albuquerque, NM 87131, USA

The detail of how to obtain the L-formulae in the main paper for the circular Petri dish and the multiple-mask set-up is as follows.

We now have, as in the analysis in the main paper, $u(x) = I\cos(\alpha|x| - \phi)$ inside the right mask, i.e., for $d < x < d + L$, but to the right of the right mask, i.e., for $x > d+L$, $u(x)$ is not proportional to $\exp(-\alpha_1|x|)$ as in the earlier analysis, but

$$u(x) = O\cosh(\alpha_1|x| - \zeta). \tag{1}$$

This expression, which, in the right region under consideration, where $x > 0$, can be written as $u(x) = O\cosh(\alpha_1 x - \zeta)$, will hold on the left extreme as well but there it simplifies to $u(x) = O\cosh(\alpha_1 x + \zeta)$. The additional phase ζ is immediately determined from the periodicity in the boundary conditions, i.e., by matching the logarithmic derivative of the solution at $|x| = d + L + R$:

$$\eta = \alpha_1(d + L + R). \tag{2}$$

Matching also at $x = \pm d$ and $x = \pm(d+L)$, one arrives at the new formula for critical L and d, valid for a *circular* Petri dish:

$$L = \sqrt{\frac{D}{a}}\Big(\arctan\Big(\sqrt{\frac{a_1}{a}}\tanh\big(R\sqrt{\frac{a_1}{D}}\big)\Big) + \\ + \arctan\Big(\sqrt{\frac{a_1}{a}}\tanh\big(d\sqrt{\frac{a_1}{D}}\big)\Big)\Big). \tag{3}$$

We see that the circular dish result, Eq. (3) here, and Eq. (10) in the main paper, is symmetric in the two hostile lengths R and d as it obviously must be, that it reduces to the result for the linear dish of infinite extent, when R becomes infinite since then the new hyperbolic tangent in Eq. (3) reduces to 1, and that, when R vanishes (equivalently when d vanishes), it yields a new expression for the critical width for the single-mask case but with twice the width value. If there were simply a single mask in a circular Petri dish of extent R and no d, the generalization of the Ludwig formula that would come out of our analysis would be

$$L = 2\sqrt{\frac{D}{a}}\arctan\Big(\sqrt{\frac{a_1}{a}}\tanh(\alpha_1 R)\Big). \tag{4}$$

Most importantly, we see that it should be possible in principle to use the new analytic result(s) for experimental probing of the phenomenon under consideration since one could construct and employ circular Petri dishes of desirable radius. Needless to say, the added effects discussed here would not be discernible for R values that are very large as then bacteria would die in the external regions quickly enough.

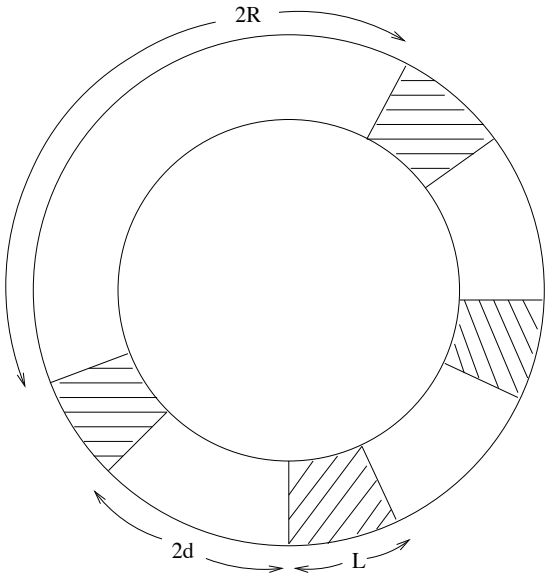

FIG. 1: The proposed set-up in a *circular* geometry shown here with a multiple mask set-up with 3 experimentally controllable parameters: R as well as L and d.

We have also derived the corresponding expressions combining circular dish geometry with the multiple mask set-ups. It is straight forward to put the two arguments together. Then, the 4-mask formula takes the form, $\mathcal{R}$ being R measured in units of $\sqrt{D/a}$,

$$\mathcal{L} = \arctan\big(\xi\tanh\xi\mathcal{R}\big) + \arctan\Big(\xi\tanh\Big(2\xi\delta - \mathrm{arctanh}\big(\\ (1/\xi)\tan(\mathcal{L} - \arctan(\xi\tanh\xi\delta))\big)\Big)\Big). \tag{5}$$

whose reduction to the linear dish formula is obvious as R becomes infinite. We have verified all these expressions that we have derived, by comparing their predictions to numerical solutions of the Fisher equation with explicit (arbitrary) non-zero b's.